Article:
Arruda, Guilherme S., Li, Juntao, Martins, Augusto et al. (3 more authors) (2020) Reducing the Surface Area of Black Silicon by Optically Equivalent Structures. IEEE Journal of Photovoltaics. 8880473. pp. 41-45. ISSN 2156-3381

https://doi.org/10.1109/JPHOTOV.2019.2945912

Reducing the surface area of black silicon by optically equivalent structures

Guilherme S. de Arruda[1], Juntao Li[2], Augusto Martins[1], Kezheng Li[3], Thomas F. Krauss[3] and Emiliano R. Martins[1]

[1]São Carlos School of Engineering, Department of Electrical and Computer Engineering, University of São Paulo, São Carlos,13566-590, São Paulo – Brazil

[2]State Key Laboratory of Optoelectronic Materials and Technologies, School of Physics, Guangzhou 510275, China

[3]Department of Physics, University of York, York, YO10 5DD, UK

Abstract

Black silicon is a promising low-cost technology to boost the efficiency of solar cells. The use of black silicon, however, is still hindered by surface recombination. This hurdle motivates the search for structures with lower surface area but similar optical properties. Here, we identify an approach for reducing the surface area of black silicon while maintaining optical performance. Specifically, we have realised that wavelength scale arrays of nano-tapers have similar anti-reflection properties as black silicon, but with less than half of the surface area. Additionally, we highlight that the light trapping properties of black silicon are not optimal and that its performance can be further improved by using nanostructures with controlled scattering properties. We quantify the optical performance of the structures and their surface area, thus identifying optically equivalent structures with reduced surface areas. We believe that these findings will help to boost the efficiency of devices based on black silicon.

1 - Introduction

Crystalline silicon (c-Si) solar cells are currently the most important technology in the photovoltaics industry. The predominance of c-Si solar cells stems from their good balance between efficiency and cost. Much of the research is driving towards improving the efficiency without incurring additional costs. The efficiency of a solar cell depends on both its optical and its electrical properties and an improvement in one area may lead to degradation in the other. An important example for such a trade-off is the use of black silicon, which has remarkable optical properties, with reflectivities close to 0 % having been reported [1,2], yet its large surface area degrades the electrical performance by increasing surface recombination. Black silicon is a particularly appealing technology, because it incurs little if any additional cost during manufacturing. Nevertheless, the efficiency of black silicon c-Si solar cells remains lower, with

22.1 % [3], than that of the benchmark PERL solar cell [4], which employs inverted pyramids for Anti-Reflection (AR) and light trapping and achieves an efficiency of 25.0 %, or 26 % for the case of the HIT cell [5].

The potential of black silicon to deliver low cost and highly efficient solar cells has driven intense research in this area. Concerning the electrical properties, the development of passivation techniques for black silicon, which is a key goal to reducing surface recombination [6,7,8], has led to a remarkable progress on black silicon based solar cells, culminating in the record efficiency of 22.1 % [2] mentioned above. The research effort on the optical side, on the other hand, has been largely focused on the development and application of numerical methods to assist the characterization of the optical properties of black silicon [9,10,11,12,13,14]. One important approach to mitigating surface recombination, however, is to the reduce the surface area of black silicon. For example, the surface area can be reduced by replacing a nano-hole textured surface by inverted pyramids, leading to an efficiency of 18.45 % in multi-crystalline silicon solar cells [15]. Here, we propose to address the problem of reducing the surface area of black silicon from the point of view of optical design. The key question we wish to address is whether the superior optical properties of black silicon can be achieved by optically equivalent structures with lower surface area. To achieve this objective, we separate the roles of antireflection and light trapping in the design, gaining insights on the relationship between these two properties for highly performing structures. In particular, we recognise that the AR properties only have very little dependence on the height of the needle-like structures that are typical of dry-etched black silicon and we identify that nearly perfect AR can be achieved with tapered nanostructures of much reduced surface area. Furthermore, we reveal that the scattering properties of black silicon structures are not optimal for light trapping and that they can be improved if tapered nanostructures with controlled scattering properties are used.

2 - Results

2.1 AR properties

In order to gain insights into the physics of anti-reflection (AR) with nanostructures, we begin by investigating the AR properties of black silicon structures and compare them to different types of engineered nanostructures. As a representative of black silicon, we chose a randomized

distribution of needle-like structures (Figure 1a), which features the two main optical properties of black silicon: graded index and random scattering. We calculate the optical properties using the Rigorous Coupled Wave Analysis (RCWA), with a square unit-cell of side length 2 μm, shown in Figure 1a, following [14]. The AR properties of this structure are compared to an optimised sub-wavelength array of 110 nm thick nano-pillars, which serve as a good model system for a nanostructured interface [16]. Both structures are placed on top of a silicon substrate, as shown in Figure 1a, and their transmission is calculated, as shown in Figure 1b. The needles exhibit nearly perfect transmission due to the graded-index layer they create between air and silicon, thus promoting optical impedance matching. An important advantage of the graded-index effect is that it is largely wavelength independent, thus leading to the broad-band high transmission seen in Figure 1b. The nano-pillars, on the other hand, act as an effective medium layer at long wavelengths (> 600 nm) and as a diffractive structure at short wavelengths (< 600 nm). The effective medium property is apparent from the high transmission at 800 nm, where the layer meets the λ/4 AR condition. The high transmission then extends further into the short wavelength regime than one might expect from a simple λ/4 layer because of the onset of diffraction (Figure 1c). For wavelengths shorter than 600 nm, the first order diffraction channel into the substrate opens up (indicated by diamonds), with a peak at 530 nm. This combination of the quarter-wavelength condition and diffraction leads to a remarkably high broad-band transmission. In order to quantify the transmission and to make it relevant for solar cells, we normalize the wavelength-dependent transmission function to the solar spectrum (AM1.5G) by defining the Integrated Solar Transmission (IST) as the percentage of solar photons that is transmitted into the substrate:

$$IST = 100 \times \frac{\int S(\lambda)T(\lambda)d\lambda}{\int S(\lambda)d\lambda} \ (\%) \qquad \text{Equation 1}$$

where $S(\lambda)$ is the photon density of the AM1.5G spectrum and $T(\lambda)$ is the transmission at the free-space wavelength λ. The IST as a function of the nano-pillar period is plotted in Figure 1d and it is apparent that the function peaks at 210 nm, with a monotonic decrease as the period is increased away from the subwavelength regime. This requirement of subwavelength periods for high transmission is analogous to the condition of perfect AR by optical resonance [17].

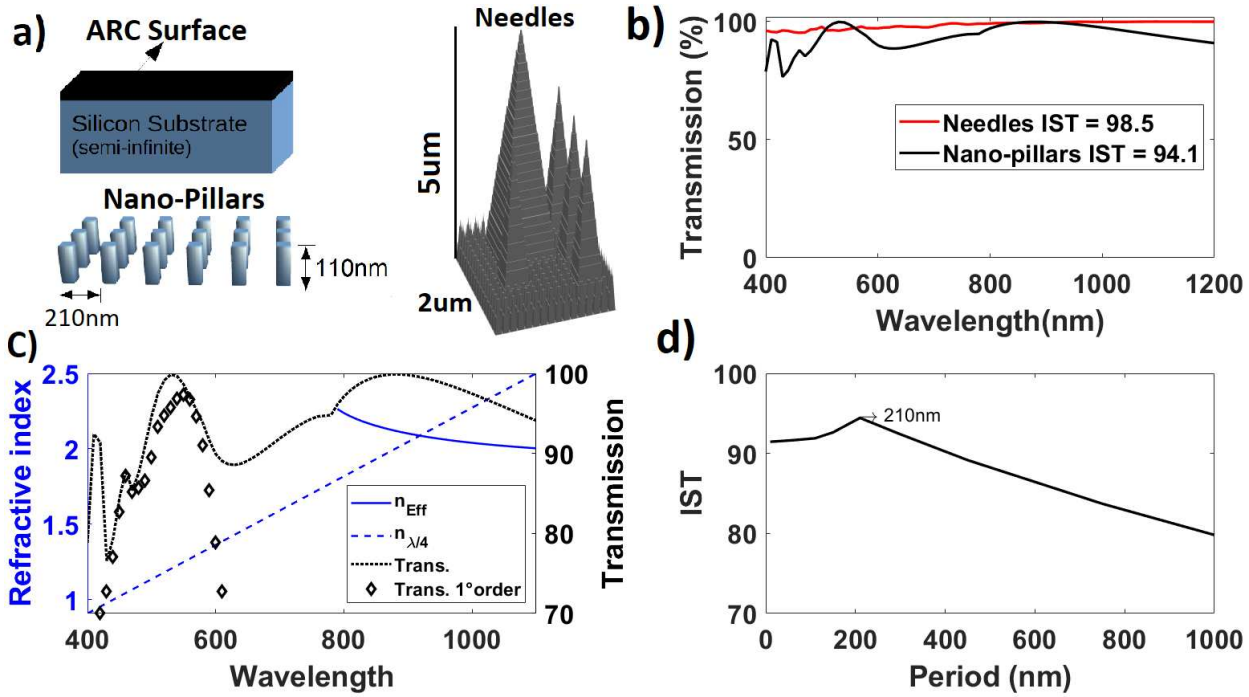

Figure 1: a) Illustration of the two structures under investigation, namely a random distribution of needle-like structures ("needles"), representing black silicon, and a subwavelength array of nano-pillars. b) Transmission of nano-pillars (black) and needles (red). c) The high transmission of the nano-pillars results from a combination of thin-film interference (matching the quarter wavelength condition at 800 nm) and the diffraction peak at 530 nm. d) The high performance of the nano-pillars depends on their period mainly because of the diffraction effect.

The IST of the needles reaches an impressive 98.5 %, whereas the IST of the nano-pillars is 94.1 %, which is still surprisingly high for such a thin structure without graded index.

We have, therefore, three distinct physical mechanisms for achieving good antireflection: a) the graded-index of the needles, b) thin-film interference and c) diffraction of the nano-pillars. These multiple mechanisms, together with the high performance of the nano-pillars, naturally leads to the question whether a combination of these effects could lead to a highly performing structure with reduced surface area. Indeed, such a combination can be straightforwardly achieved by tapering the nano-pillars, as shown in the inset of Figure 2. We assume that the optical behaviour of such nano-tapers may benefit from the advantages of all three domains. Figure 2 shows the IST of the nano-tapers for a range of aspect ratios, defined as the ratio between the height and the period of the tapers. We assume that, as in real black silicon, the tapers fill the entire surface area, hence have taken the base length to be equal to the period. Notice that ISTs above 99 % can be

achieved with this arrangement even for wavelength-scale periods. This high performance is based on the fact that the tapers soften the dependence on period observed with the nano-pillars.

Notice that, for all periods, an optimum IST is achieved for an aspect ratio of about 1.5. For short periods (below 400 nm), the IST is only slightly increased for higher aspect ratios, whereas for larger periods the IST drops for larger aspect ratios. Since a random structure can be interpreted as being comprised of a continuum of periods, these results suggest that the optimum aspect ratio of random structures should be near 1.5. This high IST for the nano-tapers is achieved with a strong reduction in surface area, which is about 2.5 times lower compared to the needles. These results show that it is possible to achieve, and even surpass, the AR properties of conventional black silicon by using nano-tapers with reduced surface area.

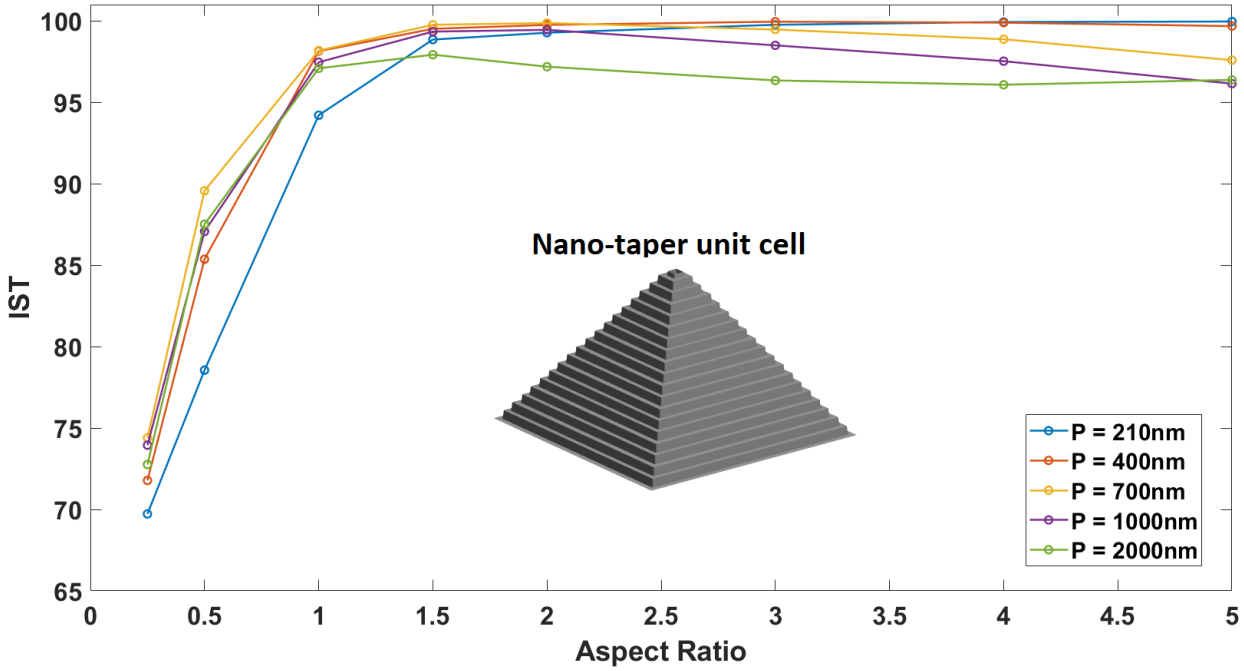

Figure 2: Integrated solar transmission (IST) of nano-taper arrays as a function of the aspect ratio for different periods. An optimum aspect ratio of 1.5 is found for all periods, indicating that this is the optimum aspect ratio for randomized structures. The IST of the nano-tapers is 1 % higher than the needles and the nano-tapers have about 2.5 times less surface area than the needles.

2.2 – Light trapping properties

So far, we have only considered the transmission/reflection at the front surface. Clearly, for a high performing solar cell, we need to ensure that the maximum amount of light enters the cell and that all of this light is absorbed and generates electron-hole pairs. To ensure maximum absorption, the light should also experience some scattering, since scattering increases the propagation length,

a phenomenon usually referred to as light trapping. The importance of light trapping depends on the actual thickness of the absorbing layer, and it is well known that thin film cells can benefit significantly from light trapping. Since all high-performing solar cells are thick-film cells, we have chosen to study a 200 μm thick silicon film in this section.

To gain insights into the role of light trapping vs. antireflection, we use four different structures: the needle-like structures of Figure 1a, the subwavelength array of nano-pillar of Figure 1a, a wavelength-scale array with period of 700 nm and a quasi-random structure with period of 1000 nm. The latter two are better suited for light trapping, as larger periods open up more diffraction channels, while the quasi-random also offers a more controlled distribution of diffraction channels [18,19,20,21].

The parameters of the wavelength-scale array and the quasi-random were found by a parametric scan to optimise for absorption. Note that none of these structures are tapered and we will revisit the benefit of tapering further down. The structures are illustrated in Figure 3a and their geometrical parameters are summarized in Table 1. Notice that we assume a thin layer of silicon nitride on top of the wavelength-scale and the quasi-random to improve their AR properties (this layer is not assumed in the other structures because it does not improve their performance).

Figure 3b shows the transmission (dashed lines) and absorption (solid lines) of the four structures on a 200 μm thick film. The overall absorption is quantified by the Integrated Absorption (ISA), defined as:

$$ISA = 100 \times \frac{\int S(\lambda)A(\lambda)d\lambda}{\int S(\lambda)d\lambda} \ (\%) \qquad \text{Equation 2.}$$

Where A is the absorption in the silicon layer. The results are summarised in Table 1.

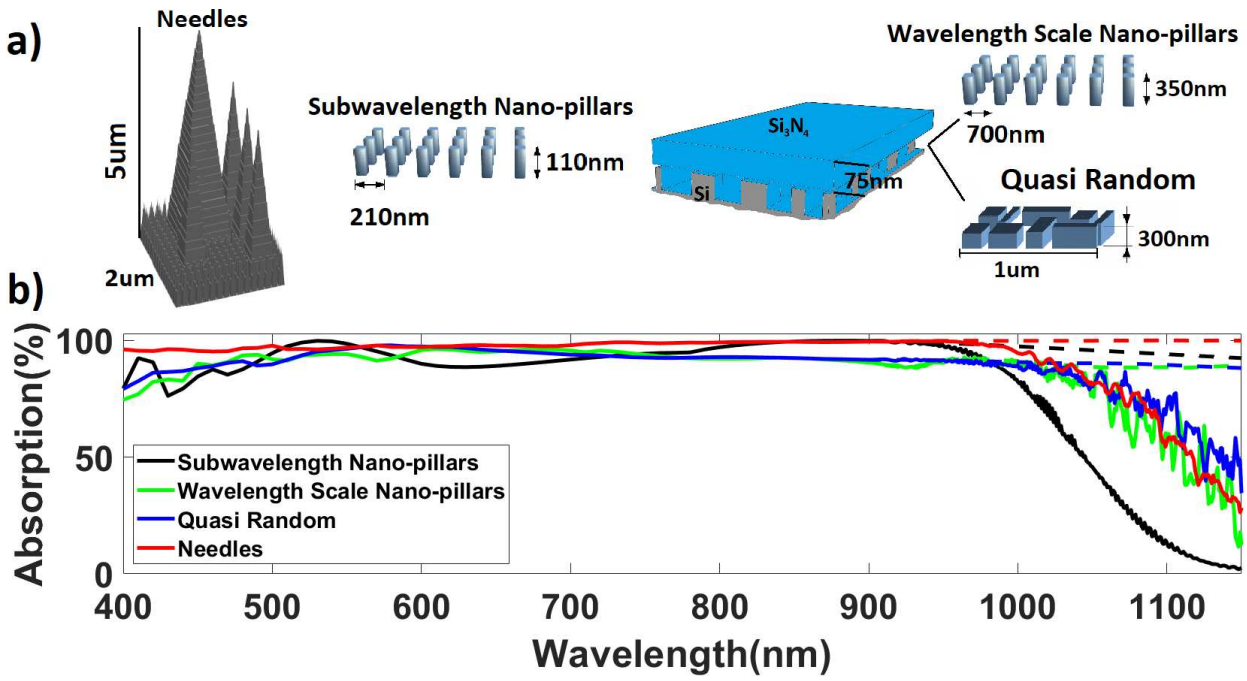

Figure 3: a) four geometries are explored for light trapping: a subwavelength array of nano-pillars, a wavelength scale array of nano-pillars, a quasi-random structure, and the randomized needle-like structure (needles). b) Transmission (dashed) Absorption (solid) of light on a 200 μm thick silicon layer with the four structures on top. The highest Integrated Solar Absorption (ISA) is reached for the needles, while the quasi-random is rather lower. Notice, however, that the difference in transmission (IST) is smaller than in absorption (ISA) indicating that the light trapping properties of the quasi-random are better. Indeed, the highest Integrated Absorption for Transmitted Photons is reached for the quasi-random, indicating better scattering properties for the latter.

A comparison between the ISA of the wavelength-scale and the subwavelength arrays highlights the importance of light trapping even in 200 μm thick c-Si films: the superior IST of the subwavelength array is not translated into a superior ISA due to the lack of diffraction in the red part of the spectrum. The high IST of the needles, on the other hand, is indeed translated into a superior ISA, since the random nature of the needles also promotes an element of scattering and light trapping.

It is well known that random and large period quasi-random structures perform better than wavelength-scale periods when broad band light trapping is required, as in thin film solar cells [18,22,23]. Thicker films, such as the 200 μm thick film of Figure 3, on the other hand, require a much narrower band for light trapping. The wavelength range where light trapping is needed can be inferred from a comparison of the absorption (solid lines) and the transmission (dashed lines)

in Figure 3b. When they coincide, at wavelengths shorter than 950 nm, all of the injected light has been absorbed, so light trapping is not required. Consequently, a 200 μm thick c-Si solar cell requires light trapping only for wavelengths between 950 and 1150 nm, which is a much narrower band than in thin-films, where light trapping is typically required for wavelengths between 500 and 1150 nm. This narrower band explains why the quasi-random has a shorter optimum period in the thicker film (period of 1 μm), than in thinner films (periods about 1.8 μm [18]).

In order to better quantify the scattering, the AR effect can be factored out by calculating the absorption with respect to transmitted photons, instead of incident photons. This can be easily done by defining the Integrated Absorption of Transmitted Photons (IATP) as:

$$IATP = 100 \times \frac{IA}{IT}(\%) \qquad \text{Equation 3}$$

This definition of IATP is convenient to give information on the separate roles of scattering and AR, as it takes into account only the transmitted photons. Table 1 shows the results for all four structures: the needles have an IATP of 92.7 % (which means that 92.7 % of the injected photons are absorbed), the quasi-random has an IATP of 95.1 % and the wavelength-scale has an IATP of 93.8 %. Therefore, both the quasi-random and the wavelength scale have an IATP larger than the needles, because of their superior light trapping properties.

Table 1: Summary of performance of the structures. S_a/P_a is the ratio of corrugated surface area (S_a) to planar surface area (P_a).

Structure	ISA	IST	IATP	Height (nm)	Period (nm)	S_a / P_a
Subwavelength Nano-pillars	82.1%	94.1%	87.2%	110	210	3.1
Wavelength Scale Nano-pillars	86.3%	92.0%	93.8%	350	700	3
Quasi-Random	87.8%	92.4%	95.1%	350	1000	4.8

Needles	91.3%	98.5%	92.7%	5000 (max)	2000	7.8

The superior scattering properties of the quasi-random and the wavelength-scale structures suggest the question whether tapered structures with controlled diffraction could be superior to the needles in terms of overall absorption. To address this question, we calculated the transmission and absorption of all four structures, but now including a taper on all structures, as illustrated in Figure 4a. The optical properties are shown in Figure 4b and the results are summarized in Table 2.

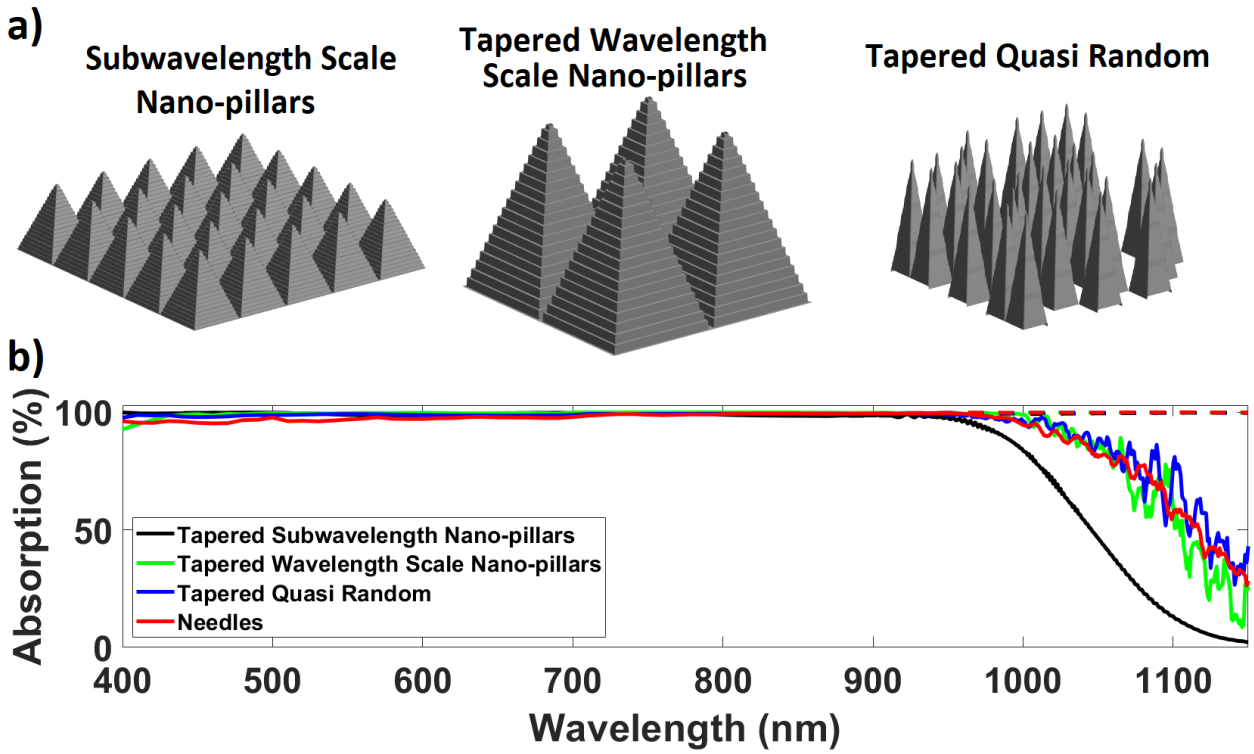

Figure 4 a) Tapered nanostructures. b) Transmission (dashed) and Absorption (solid) of tapered nanostructures

Table 2: Summary of performance of the tapered structures. S_a/P_a is the ratio of corrugated surface area (S_a) to planar surface area (P_a).

Tapered Structure	**ISA**	**IST**	**IATP**	**Height (nm)**	**Period (nm)**	**S_a / P_a**

Subwavelength Nano-pillars	86.4%	99.3%	87.0%	420	210	4.1
Wavelength Scale Nano-pillars	92.3%	99.7%	92.6%	1050	700	3.1
Quasi-Random	93.0%	99.2%	93.7%	700	1000	5.6
Needles	91.3%	98.5%	92.7%	5000 (max)	2000	7.8

As expected, the enhanced transmission of the tapered structures boosts the absorption of all structures, but now the ISA of the quasi-random is 93 % and the ISA of the wavelength scale is 92.3 % – both larger than the 91.3 % of the needles.

This superior absorption is a consequence of a significant increase of the transmission due to tapering, which shows that the combination of the excellent AR properties of nano-tapers with controlled scattering can result in highly efficient structures with reduced surface area. The nano-tapers are optically equivalent to the needles, as they show similar (if not better) transmission and absorption properties.

3 - Conclusion

We have shown that it is possible to reduce the surface area of black silicon structures by using optically equivalent structures with lower surface area. We found that the absorption of needle-like structures that are typical of black silicon can actually be improved using structures with lower surface area, by combining the excellent AR properties of nano-tapers with controlled scattering. These results and insights are an important guide in the research on black silicon structures with reduced surface recombination.

.

Funding Agencies:

São Paulo Research Foundation (FAPESP): grant# 2016/05809-0, grant# 2015/21455-1.

REFERENCES

1 Otto, Martin, et al. "Black silicon photovoltaics." Advanced optical materials *3.2 (2015): 147-164.*

2 Steglich, Martin, et al. "An ultra-black silicon absorber." *Laser & Photonics Reviews* 8.2 (2014): 13-L17.

3 Savin, Hele, et al. "Black silicon solar cells with interdigitated back-contacts achieve 22.1% efficiency." Nature nanotechnology *10.7 (2015): 624.*

4 Green, Martin A. "The path to 25% silicon solar cell efficiency: history of silicon cell evolution." Progress in Photovoltaics: Research and Applications *17.3 (2009): 183-189.*

5 Yoshikawa, Kunta, et al. "Silicon heterojunction solar cell with interdigitated back contacts for a photoconversion efficiency over 26%." Nature Energy *2.5 (2017): 17032.*

6 Otto, Martin, et al. "Extremely low surface recombination velocities in black silicon passivated by atomic layer deposition." Applied Physics Letters *100.19 (2012): 191603.*

7 Wang, Wei-Cheng, et al. "Surface passivation of efficient nanotextured black silicon solar cells using thermal atomic layer deposition." ACS applied materials & interfaces *5.19 (2013): 9752-9759.*

8 Oh, Jihun, Hao-Chih Yuan, and Howard M. Branz. "An 18.2%-efficient black-silicon solar cell achieved through control of carrier recombination in nanostructures." Nature nanotechnology *7.11 (2012): 743.*

9 Kroll, Matthias, et al. "Optical modeling of needle like silicon surfaces produced by an ICP-RIE process." Photonics for Solar Energy Systems III*. Vol. 7725. International Society for Optics and Photonics, 2010.*

10 Ma, Shijun, et al. "A theoretical study on the optical properties of black silicon." AIP Advances *8.3 (2018): 035010.*

11 Bett, Alexander Jürgen, et al. "Wave optical simulation of the light trapping properties of black silicon surface textures." Optics express *24.6 (2016): A434-A445.*

12 Ravindra, N. M., S. R. Marthi, and S. Sekhri. "Modeling of optical properties of black silicon/crystalline silicon." Silicon. J. Sci. Ind. Metrol. *1.1 (2015): 100001*

13 Elsayed, Ahmed A., et al. "Optical modeling of black silicon using an effective medium/multi-layer approach." Optics express *26.10 (2018): 13443-13460.*

14 Bett, Alexander Jürgen, et al. "Wave optical simulation of the light trapping properties of black silicon surface textures." Optics express *24.6 (2016): A434-A445.*

15 Ye, Xiaoya, et al. "18.45%-Efficient multi-crystalline silicon solar cells with novel nanoscale pseudo-pyramid texture." Advanced Functional Materials *24.42 (2014): 6708-6716.*

16 Proust, Julien, et al. "Optimized 2D array of thin silicon pillars for efficient antireflective coatings in the visible spectrum." Scientific reports *6 (2016): 24947.*

17 Wang, Ken Xingze, et al. "Condition for perfect antireflection by optical resonance at material interface." Optica *1.6 (2014): 388-395.*

18 Martins, Emiliano R., et al. "Deterministic quasi-random nanostructures for photon control." Nature communications *4 (2013): 2665.*

19 Martins, Emiliano R., et al. "Engineering gratings for light trapping in photovoltaics: The supercell concept." Physical Review B *86.4 (2012): 041404.*

20 Li, Kezheng, et al. "High speed e-beam writing for large area photonic nanostructures—a choice of parameters." Scientific reports *6 (2016): 32945.*

21 Li, Juntao, et al. "Spatial resolution effect of light coupling structures." Scientific reports *5 (2015): 18500.*

22 Oskooi, Ardavan, et al. "Partially disordered photonic-crystal thin films for enhanced and robust photovoltaics." Applied Physics Letters *100.18 (2012): 181110.*

23 Vynck, Kevin, et al. "Photon management in two-dimensional disordered media." Nature materials *11.12 (2012): 1017.*